Effect of geometry and thermal mass of Direct-Metal-Laser-Sintered aluminium heat exchangers filled with Phase Change Materials on Lithium-Ion cells' passive cooling

Effect of geometry and thermal mass of Direct-Metal-Laser-Sintered aluminium heat exchangers filled with Phase Change Materials on Lithium-Ion cells' passive cooling

Dr S. Landini[*,1], W. Delgado-Diaz[2], R. Ravotti[2], R. Waser[3], Dr A. Stamatiou[2], Prof. J. Worlitschek[2], Prof. T. S. O'Donovan[1]

[1]Institute of Mechanical, Process and Energy Engineering, School of Engineering and Physical Sciences, Heriot-Watt University, Edinburgh EH14 4AS, United Kingdom

[2]Thermal Energy Storage Research Group, Lucerne University of Applied Sciences and Arts (HSLU), CH-6048 Horw, Switzerland

[3] Cowa Thermal Solutions AG, Technopark Lucerne, Platz 4, CH-6039 Root D4, Switzerland

Abstract

This study investigates the effect of mass and geometry as design parameters of a Lithium-Ion (Li-Ion) cell Thermal Management System (TMS) based on a Direct-Metal-Laser-Sintered (DMLS) structure filled on Phase Change Material (PCM). As part of a TMS, complex heat exchanger geometries are produced using DMLS technique, filled with a PCM, and experimentally tested using an established methodology. The design parameters investigated are PCM mass and DMLS heat exchanger geometry to assess the effects of increased thermal energy storage capacity and enhanced equivalent thermal conductivity respectively on the overall performance of a Li-Ion pouch cell. Constant discharge rate tests and stress sequences are used to reproduce realistic Li-Ion cell operating conditions. It has been shown that all PCM TMS effectively improve the isothermalisation of the cell under a single discharge at rate 3C compared to natural convection and decreased the cell maximum temperature by at least 5°C. The enhanced heat transfer performance of finned designs further improves the temperature uniformity and decreases the cell maximum temperature. When tested under stress sequences, the TMS characterised by a higher thermal mass maintained functional isothermalisation for 5 cycles; this is an increase of two cycles than for the TMS with a lower thermal mass. By using a Pareto front analysis based on thermal and geometrical variables, specific designs are indicated as the best combination of thermal performance and additional weight for single discharge tests (i.e., intermittent load) and stress sequences (i.e., constant load).

Keywords: Li-Ion cell; thermal management systems; PCM; latent heat; iso-thermalisation; design criteria

* Corresponding Author:
s.landini@hw.ac.uk (S. Landini)

Contents

Glossary

CR	Charge Rate	LDPE	Low-Density Polyethylene
DR	Discharge Rate	OCV	Open Circuit Voltage
EOL	End of Life	PCM	Phase Change Material
DAQ	Data Acquisition	PGS	Pyrolytic Graphite Sheets
DOD	Depth of Discharge	PHS	Pump Hydro Storage
EESS	Electrical Energy Storage System	SMU	Source Measure Unit
EG	Expanded Graphite	TCE	Thermal Conductivity Enhancement
EV	Electric Vehicle	TMS	Thermal Management System

1. Introduction

Li-Ion cells are electro-chemical devices typically employed as electricity storage systems in stationary applications and are key to the performance of electric vehicles [1–5]. Their performance, however, is highly sensitive to average operating temperature and temperature uniformity [1,6,7]. Therefore, a thermal management system (TMS) is required to maintain an isothermal condition for their entire operating life. To do so, several techniques have been proposed in previous literature [1]. It has been established that Phase Change Materials (PCM) have great potential as part of a low-cost and passive TMS [1,2,8–12].

In a previous study [4], a novel Direct-Metal-Laser-Sintered (DMLS) aluminium Heat Exchanger (HEX) filled with octadecane as the PCM was proposed as a passive TMS for Li-Ion cells. Here, a new methodology based on heat flux measurements to analyse Li-Ion cells' electrical, thermal, and electrochemical performance was introduced. The study focused on both Li-Ion cells' single discharges to emulate intermittent loads, and consecutive charge-discharge cycles without resting periods to emulate constant loads. The Li-Ion cell's surface temperature rise and surface temperature uniformity were measured to evaluate the TMS performance. During single discharges, the temperature rise was lower and uniformity was improved than for the air natural convection when using the proposed PCM DMLS HEX. Moreover, under consecutive cycles, the peak temperature rise was reduced by 5°C. Most importantly, results showed that the optimal design of a PCM HEX is case dependent and when considering a real application, the actual cycling characteristics of the specific Li-Ion cell must be carefully considered.

The first study focused on the performance of a simple geometry to improve the thermal conditions and in-cell temperature uniformity during operation of a Li-Ion cell. Geometry and size of the TMS were identified as key parameters during this stage, and therefore, the novelty of the present study remains in further characterising the particular effects of thermal mass (PCM mass fraction) and geometry (PCM thermal conductivity enhancement methods using aluminium fins).

Hence, this research investigates the effect of important design parameters, being the mass of PCM and geometry of the aluminium HEX structure, on the performance of PCM DMLS HEX as passive TMS for Li-Ion cells. Four HEX geometries based on the benchmark design proposed in the above-mentioned study [4], are designed, manufactured, and tested to evaluate the separate and joint effect of HEX geometry and TMS thermal mass on the TMS ability to maintain the isothermal operation of a Li-Ion cell. As proposed by Landini et al. [4], both intermittent (single discharges at DR=3C) and constant (consecutive charge-discharge cycles at CR=1C,

DR=3C) electrical loads are tested. The HEXs external walls are insulated to guarantee a consistent thermal boundary condition for all tests and to emulate the typical heat convection depletion which a single cell experiences when installed within a battery pack. The isothermalisation effectiveness of the PCM DMLS HEXs is also compared to a natural convection boundary condition.

Overall, the PCM DMLS HEX are designed to be highly conductive enclosures for PCM to provide Li-Ion cell isothermal conditions and to reduce cell temperature rise for both intermittent and constant loads.

2. Methodology

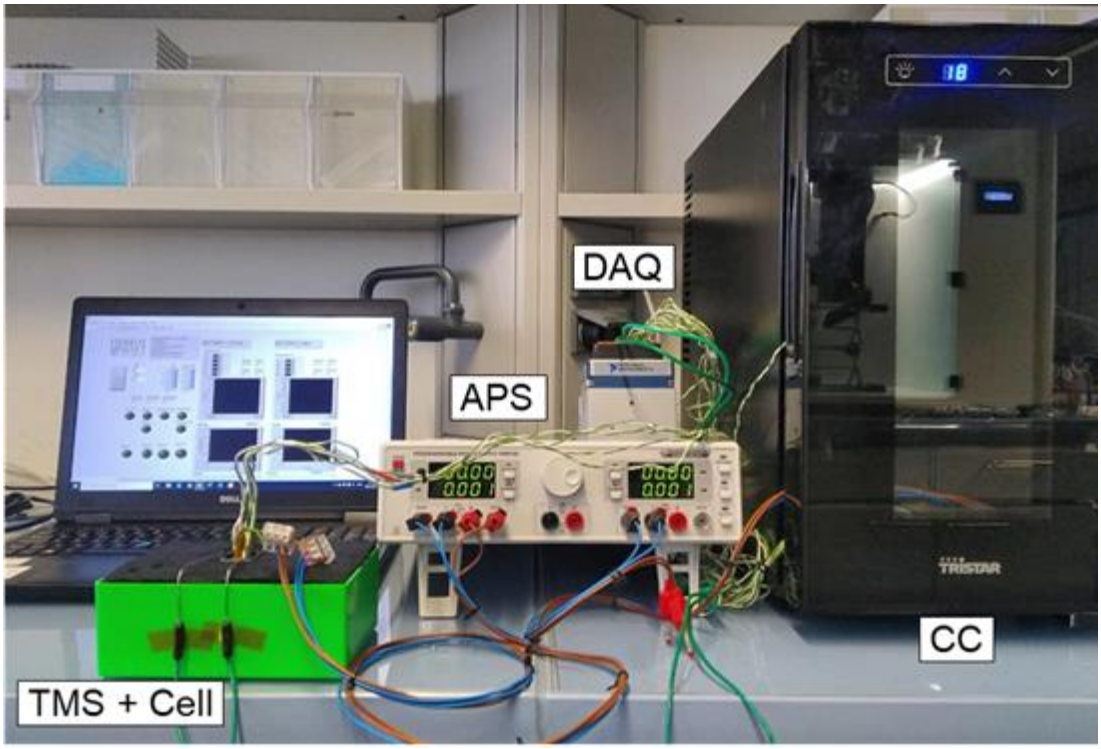

Figure 1: Experimental Test Rig at HSLU, as employed in [4]. Legend: TMS=Thermal Management System, APS=Arbitrary Power Supply, DAQ=Data Acquisition system, CC=Cooling Chamber.

Figure 1 shows the main components of the experimental test rig at HSLU, as reported by Landini et al [4]. The Li-Ion cells are cycled using a programmable Arbitrary Power Supply (APS in Figure 1), which is employed as a power supply (Li-Ion cell charge) and an electronic load (Li-Ion cell discharge). The APS measures the cell's current and voltage. A cooling chamber (CC in Figure 1) is used to keep a fixed surrounding temperature. A National Instruments Data Acquisition system (DAQ in Figure 1) in connection with thermal sensors and a dedicated LabVIEW code is used to control the entire test rig. More details can be found in Landini et al [4].

Table *1* reports the electrical and geometric details of the Li-Ion pouch cells used throughout the tests conducted in this study. The cells were electrically and thermally characterised at Heriot-Watt University (HWU) using a novel test rig and methodology established by Landini and O'Donovan [13]. The novel HWU test rig emulates an active TMS and it comprises a thermal chamber, a micro wind tunnel, and a control system. A thermal boundary condition is imposed on the cell's surface where the heat transfer coefficient is kept constant and, by dynamically tuning the chamber temperature to control the temperature difference between cell and cooling medium, a dynamic surface heat flux balances the unstable cell heat generation rate. This guarantees a constant cell surface temperature both temporally and spatially. Importantly, this is significantly different from a standard uniform environmental condition (defined as isoperibolic) where the surface temperature and critically the rate of heat transfer from the cell would be significantly different from an active TMS. More details can be found in Landini and O'Donovan [13].

The results of the characterisation are reported in section 3.1. The Li-Ion cells were subject to different electrical regimes of charge and discharge cycles employing an HM8143 Arbitrary Power Supply (APS) (Table 2) used as both a power supply for the charge phase or an electronic load for the discharge phase. The temperature profiles in the system were captured using K-Type thermocouples inside and around the TMS connected to a National Instruments data acquisition system (DAQ).

Table 1: Li-Ion cell properties

Component	**Li-Ion Cell**
Brand	RENATA
Model	ICP422339PR
Technology	Li-Ion Polymers
Voltage [V]	3.7
Capacity [mAh]	330
Height [mm]	40
Width [mm]	23.5
Thickness [mm]	4.6
Mass [g]	7.3
Density [kg/m3]	1667

Table 2: Arbitrary Power Supply properties, as employed in [4]

Component	**Arbitrary Power Supply**
Name	R&S®HM8143
Voltage [V]	0-30
Current [A]	0-2
Power [W]	0-60
Power Supply Mode	Charge CC-CV

Power Sink Mode	Discharge CC
Power Connectors	4mm Banana Type
Sensing Connectors	4mm Banana Type
Digital Interface	RS-232/USB

The PCM employed for this study was a bio-based water-insoluble organic compound, provided by CrodaTherm Ltd. The main properties of the PCM were assessed at the analytic lab of the Competence Centre of Thermal Energy Storage (CCTES) of HSLU. The PCM was measured between 0 – 40°C in a METTLER TOLEDO (Columbus, OH, USA) DSC 3+ equipped with autosampler previously calibrated with indium standards. First, two heating-cooling cycles at 10K/min were performed to precondition the samples as suggested by Muller et al. [14], followed by three consecutive heating-cooling cycles at 0.5K/min. The curves at 10K/min were not used to evaluate the properties of the PCM. The analysis was repeated three times; each time with a new sample of CrodaTherm21, for a total of nine consecutive repetitions. The averages of the results are reported in Table *3*.

The PCM DMLS HEX were composed of blocks of aluminium produced by Direct-Metal-Laser-Sintering (DMLS) as reported by Landini et al. [4]. The metal powder used in the DMLS process was a Concept Laser CL31AL and made of 86% aluminium and 10% silicium. According to datasheets from the supplier, the equivalent thermal conductivity of this powder is 120-180 W/mK.

Table 3: Phase Change Material thermo-physical properties based on nine repetitions of DSC test at a heating rate of 0.5K/min. In brackets are the standard deviations. The thermo-physical properties signed by an asterisk are taken from the manufacturer datasheet.

Property	**Unit**	**PCM CrodaTherm 21**
Category	-	Bio-based
Melting Onset	[°C]	21.2 (0.1)
Melting Peak	[°C]	22.5 (0.2)
Melting Endset	[°C]	22.9 (0.2)
Melting Gravimetric Latent Heat	[kJ/kg]	172.4 (1.0)
Solidification Onset	[°C]	20.5 (0.2)
Solidification Peak	[°C]	19.9 (0.1)
Solidification Endset	[°C]	19.5 (0.1)
Solidification Gravimetric Latent Heat	[kJ/kg]	171.7 (1.2)
Solid Thermal Conductivity *	[W/m K]	0.18
Solid Specific Heat Capacity *	[J/kg K]	2300
Solid Density *	[kg/m3]	891
Liquid Thermal Conductivity *	[W/m K]	0.15
Liquid Specific Heat Capacity *	[J/kg K]	1900
Liquid Density *	[kg/m3]	850

Four geometric designs were proposed as the evolution of the simple model reported by Landini et al [4], as illustrated in Figure 2. All designs are characterised by different geometries and TMS thermal energy storage

potential. The latter was accomplished by variation of the Aluminium and/or PCM masses, leading to different PCM mass fraction $\left(\frac{m_{PCM}}{m_{TMS}}\right)$ and relative TMS mass compared to the Li-Ion cell mass $\left(\frac{m_{TMS}}{m_{cell}}\right)$. For each design, the PCM is located within the lateral pockets while the Li-Ion pouch cell which is centrally located, as in the simple model (S) [4]. Thermal oil, Rhodorsil 47V10 has been used to ensure uniform, and consistent thermal contact between the Li-Ion cell and HEX for all tests, minimising the thermal contact resistance, compared to a thermal paste as employed in [4]. The mass of Aluminium and PCM for all four designs are reported in Table 4. The ideal TMS maximum theoretical thermal energy storage $Q_{\Delta T=10K}$, assuming a temperature rise of 10 K throughout the PCM melting temperature range, is also reported for all designs. All tests have been conducted locating the PCM HEX TMS or the single cell within a Tristar WR-7508 cooling chamber (CC) which kept a constant surrounding temperature of 17°C ± 0.1°C. All PCM DMLS HEXs were thermally-insulated by enclosing them within an ethylene-propylene rubber foam box of size 70 mm × 75 mm × 100 mm and thermal conductivity evaluated at 25°C of 0.037 W/m K, as reported in [4]. The foam was employed to thermally insulate the bottom and sides of the TMS, leaving the top exposed to the surrounding air. This was done to emulate the natural convection depletion on a Li-Ion cell's bottom and sides within a battery pack while leaving the cell's top to exchange heat with the surrounding air by natural convection, as present in commercial battery packs.

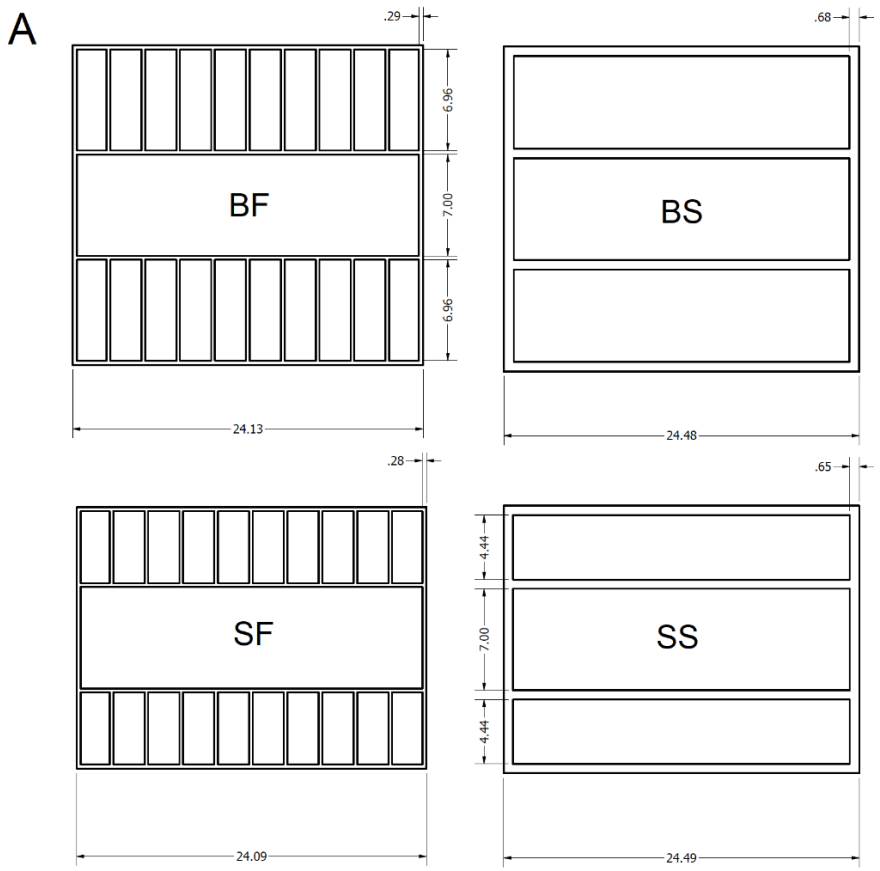

B

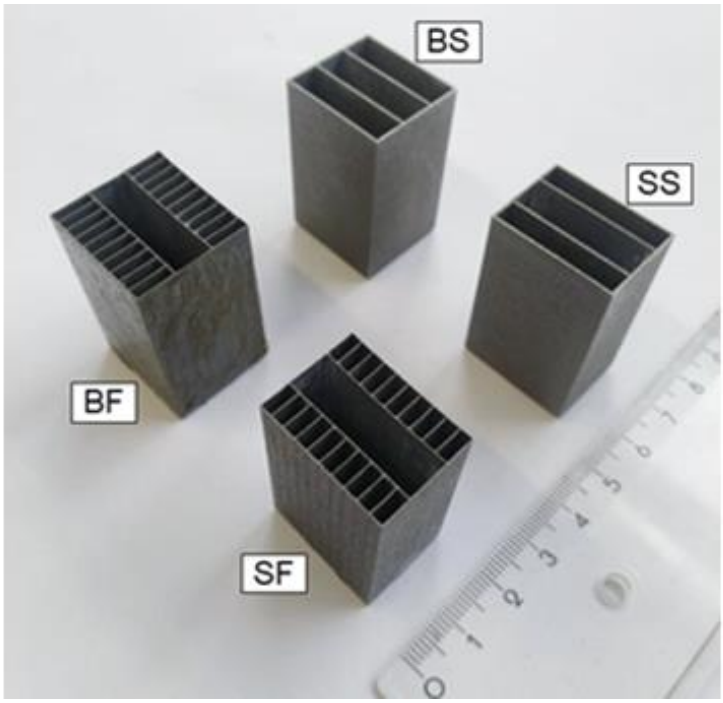

Figure 2: A. Detailed top view of the DMSL PCM Heat Exchanger Designs with dimensions reported in mm: Small Simple SS (bottom right), Small Finned SF (bottom left), Big Simple BS (top right), Big Finned (top left). Consistent height of 40mm for all designs. B. Picture of the PCM Heat Exchanger Designs. Li-Ion cell is located in the middle pocket and the PCM in the lateral pockets.

Single discharge tests at DR=3C (chosen as representative of a fast electrical regime for stationary application and typical for automotive) and 10 consecutive charge-discharge cycles at CR=1C DR=3C were conducted. The cell's voltage, current, and surface temperatures (four sensors T_1, T_2, T_3, T_4) were sampled to calculate the following cells factors:

- discharged capacity
- discharged electrical energy (E)
- average surface temperature ($T_{av} = \frac{T_1+T_2+T_3+T_4}{4}$)
- maximum surface temperature ($T_{max} = \max_{i=1,2,3,4} T_i$)
- minimum surface temperature ($T_{min} = \min_{i=1,2,3,4} T_i$)
- surface temperature uniformity ($\Delta T = T_{max} - T_{min}$)

All components of the test rig were controlled by a LabVIEW code. Samples were taken every 4 seconds (i.e. sampling rate of 0.25 Hz). The uncertainty analysis of the entire experimental rig is established by Landini et al. [4] and also reported in Table 5.

Table 4: Design characteristics of the four TMS investigated

Properties	SS	SF	BS	BF
m_{TMS} [gr]	13.46	11.69	17.70	15.89
m_{Al} [gr]	7.72	4.41	8.20	5.59
m_{PCM} [gr]	5.74	7.29	9.51	10.29
$\frac{m_{PCM}}{m_{TMS}}$	43%	62%	54%	65%
$\frac{m_{TMS}}{m_{cell}}$	184%	160%	243%	218%
$Q_{\Delta T=10K}$[J]	1110	1409	1839	1991

Legend: SS=Small Simple, SF=Small Finned, BS=Big Simple, BF=Big Finned

Table 5: Test Rig Uncertainty [4]

Quantity	Unit	Value
Temperature (T)	K	0.22
Average Temperature (T_{av})	K	0.11
Temperature Uniformity (ΔT)	K	0.31
Length (L)	mm	0.01
Area (A)	mm^2	2.13
Mass (m)	gr	0.10
Voltage (V)	mV	10.84
Current (I)	mA	5.30
Power (P)	mW	27.6

3. Results

3.1 Li-Ion cell Characterisation

The Li-Ion cell used in this study was extensively characterised both electrically and thermally under different controlled isothermal conditions (uniform constant surface temperature T_{cell}**)** and discharge rates (DR) at Heriot-Watt University by using a novel isothermalisation test rig and the Li-Ion cells characterisation methodology proposed by Landini and O'Donovan in [13]. Single constant current discharge tests at DR=1C, 3C, 5C were conducted imposing different cell uniform surface temperature from 0°C up to 50°C (step 5°C). The results are reported in Figure *3* and Table 6.

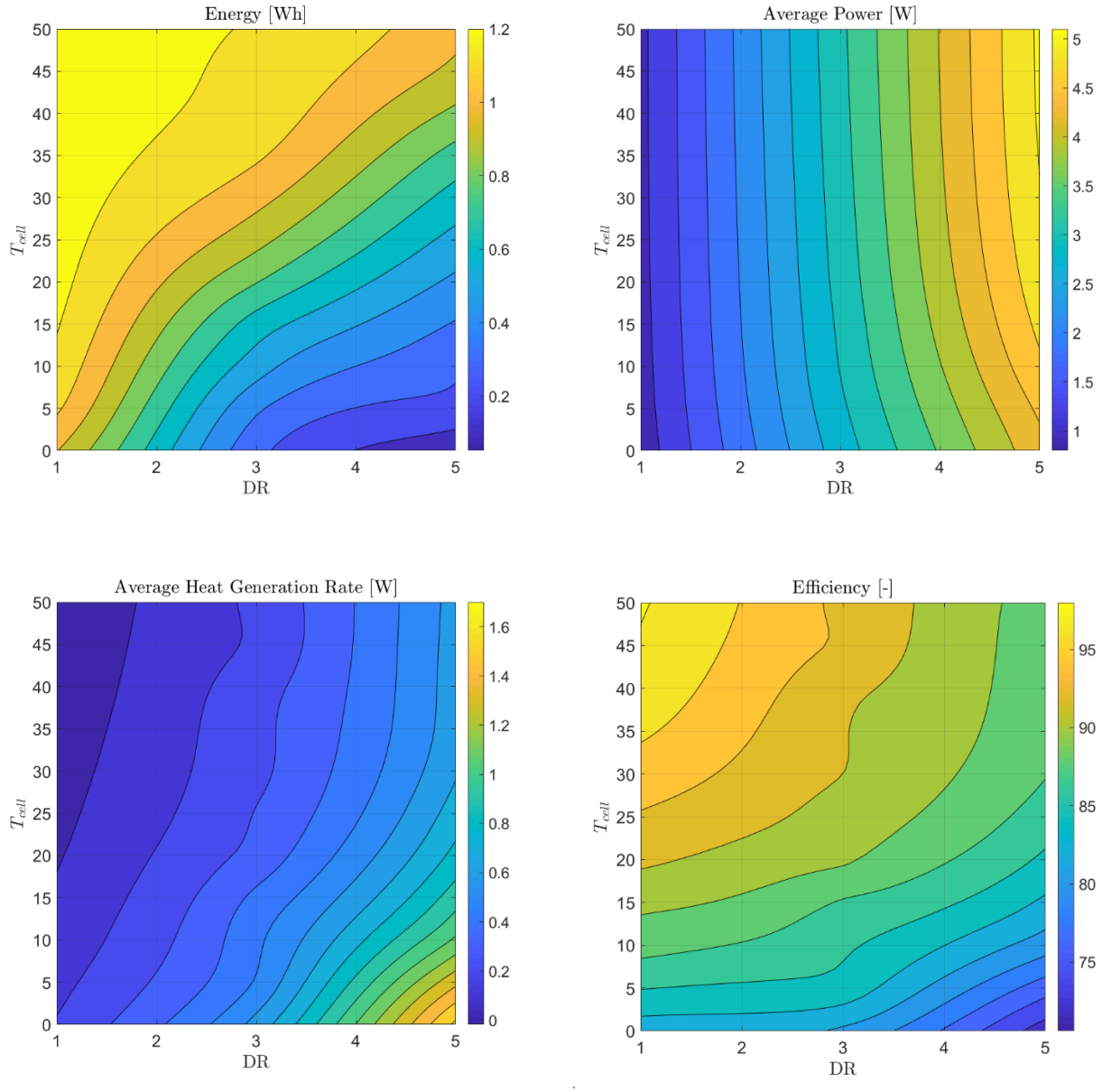

Figure 3: Li-Ion cell Characterisation under Isothermal Conditions.

Table 6 and Figure 3 clearly show that the Li-Ion cell discharges less capacity and energy at higher DRs and lower cell temperatures. This is due to the higher ohmic voltage drops which increase quadratically and linearly with the discharge current (i.e. DR) and cell resistance (typically higher at lower temperatures) respectively. As the Li-Ion cell heat generation rate is mostly proportional to the heat losses by Joule effect [1], they are expected to increase with the DR and decrease with the cell temperature as it is evident from Table 6. Consequently, the electrochemical efficiency, η decreases with the DR and increases with the cell temperature.

Table 6: Li-Ion cell characterisation under isothermal conditions

DR	T_{cell}	Capacity	Energy	Power	Heat Generation	Heat Generation Rate	η
-	[°C]	[mAh]	[Wh]	[W]	[mWh]	[mW]	-
1	0	295	1.004	1.019	207	210	82.9%
1	5	316	1.116	1.057	180	171	86.1%
1	10	326	1.173	1.078	149	137	88.7%
1	15	331	1.208	1.093	127	115	90.5%
1	20	335	1.233	1.104	102	91	92.4%
1	25	336	1.248	1.111	82	73	93.8%
1	30	337	1.258	1.116	65	58	95.1%
1	35	338	1.264	1.120	49	44	96.3%
1	40	338	1.268	1.122	37	32	97.2%
1	45	334	1.252	1.123	28	25	97.8%
1	50	337	1.265	1.125	23	20	98.2%
3	0	105	0.331	2.836	74	638	81.6%
3	5	128	0.418	2.936	73	510	85.2%
3	10	163	0.547	3.014	87	479	86.3%
3	15	193	0.654	3.056	91	424	87.8%
3	20	233	0.805	3.103	87	334	90.3%
3	25	268	0.933	3.132	91	305	91.1%
3	30	294	1.033	3.158	90	275	92.0%
3	35	315	1.114	3.181	96	274	92.1%
3	40	326	1.159	3.200	94	261	92.5%
3	45	328	1.174	3.216	79	218	93.7%
3	50	331	1.190	3.230	83	226	93.5%
5	0	44	0.128	4.397	47	1623	73.0%
5	5	87	0.263	4.558	79	1373	76.9%
5	10	101	0.320	4.741	75	1117	80.9%
5	15	121	0.392	4.869	77	956	83.6%
5	20	144	0.479	4.968	80	832	85.6%
5	25	169	0.568	5.033	85	750	87.0%
5	30	195	0.661	5.082	89	688	88.1%
5	35	223	0.761	5.112	98	656	88.6%
5	40	256	0.877	5.136	111	649	88.8%
5	45	284	0.975	5.147	122	643	88.9%
5	50	300	1.030	5.152	127	636	89.0%

Overall, evidence suggests that the most critical operating conditions for a Li-Ion cell are when it is discharged at high DR and low cell temperatures. However, the duration of each discharge cycle decreases with the DR. Therefore, while higher DRs lead to higher average heat generation rates (W), they do not necessarily lead to higher overall heat generation (Wh). Also, for context, it is important to note that DRs in the range of 1C-3C can

exemplify a stationary electrical energy storage system and mobile appliances (e.g. mobile phones, laptops) discharge regime, while that DRs in the range of 3C-5C can be representative of power tools and electric vehicles discharge load [1]. Therefore, in this study, results will be provided for DR=3C as it represents both applications.

3.2 Effect of Geometry

Figure 4 shows the maximum temperature profiles of the Li-Ion cell during a single discharge at DR=3C (upper) and the stress test comprising 10 consecutive cycles with charge at CR=1C and discharge at DR=3C (lower) for two different geometries: small simple (blue) and small finned (red). The test conducted with no dedicated TMS (i.e. in air under natural convection) is also shown as a reference (black). For the single discharge tests, the maximum temperature is plotted against the Depth Of Discharge (DOD), which is a variable commonly used in electrochemistry and is equal to the ratio between the capacity discharged and the nominal capacity. The DOD is used as a non-dimensional time to compare tests of different durations. The single discharge tests have been repeated for each design nine times and the standard deviation of the maximum temperature profiles has been computed and used as semi-amplitude of the shadowed area in Figure 4 (upper). The stress tests have been repeated 3 times and similar standard deviations have been confirmed. However, they are not reported in Figure 4 for image clarity. The same criteria are applied in the following sections.

As shown in Figure 2, the small finned design is characterised by a system of fins on the cell's wider sides which encapsulate the PCM in smaller sections, improving its equivalent thermal conductivity. Overall, the small finned design leads to a lower maximum temperature (Figure 4 upper) and a better temperature uniformity during the single discharge compared to the small simple design. The observed maximum temperature T_{max} and temperature uniformity ΔT were 22.2°C/1.2°C and 21.4°C/1.1°C for small simple and small finned designs respectively. Importantly, the maximum temperature (i.e. hotspot) was consistently located in correspondence of the cell's anode tab connector, a feature observed throughout all tests conducted in the present study. It must be pointed out that both models improved the isothermalisation of the cell compared to natural convection, where maximum temperature T_{av} and temperature uniformity ΔT were 27.2°C/1.8°C Therefore, it could be concluded that the addition of fins improved the cooling rate of the Li-Ion cells at DR=3C. Importantly, the presence of fins also leads to better temperature uniformity, an important factor in reducing degradation and extending the life of the cell.

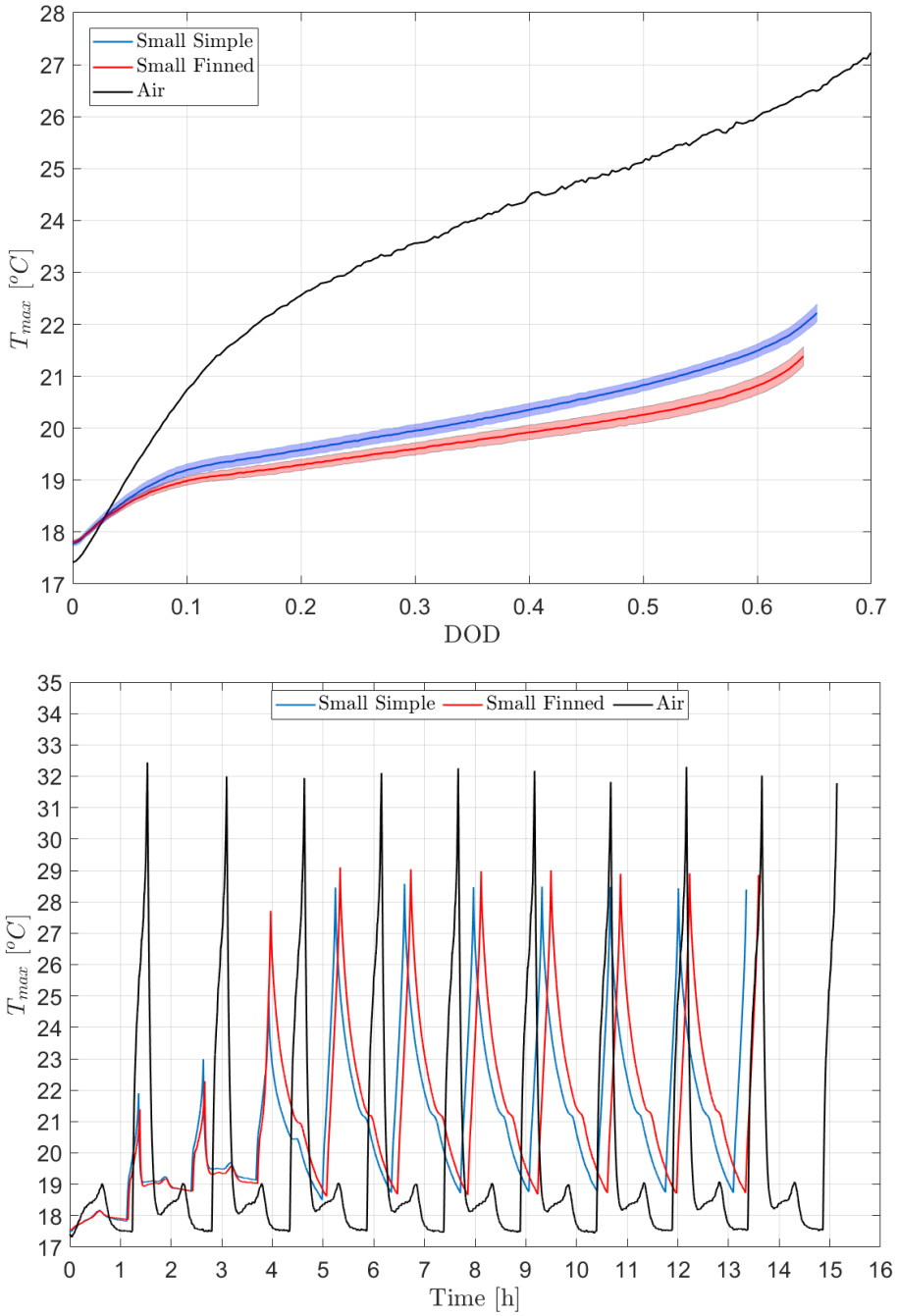

Figure 4: Effect of PCM DMLS TMS geometry (Small Simple vs Small Finned) on Li-Ion cell maximum temperature for single discharge at DR=3C (upper) and stress test comprising 10 consecutive cycles with charge at CR=1C and discharge at DR=3C (lower). The tests conducted with no dedicated TMS (i.e., air natural convection) is shown as a reference.

Results from 10 consecutive charge-discharge cycles (Figure 4 lower) at CR=1C and DR=3C allow similar conclusions can be made. Both designs effectively reduced operating temperature and the PCM was observed to go through its melting phase (first three cycles). Once the PCM lost all the latent heat and entered a liquid sensible phase, the cell temperature rose and oscillated between two definite values (19°C, 29°C), a behaviour

reported previously [4]. There was no appreciable difference between the two designs apart from the temperature oscillation range which was 0.53K higher for the small finned design. Again, both models improved the isothermalisation of the cell compared to natural convection, the latter causing the maximum temperature of the cell to oscillate in the range of 18°C-32°C and the temperature uniformity to reach 2.3°C.

3.3 Effect of thermal mass

Similar data are reported in Figure 5 for two different geometries: small simple (blue) and big simple (green). The test conducted with no dedicated TMS (i.e. air natural convection) is also shown as a reference (black). As shown in Figure 2, the “big simple” design is characterised by a higher PCM mass (i.e., thermal mass) compared to the “small simple” design due to the wider lateral pockets where the PCM is located. Overall, the big simple design leads to a similar maximum temperature (Figure 5 upper) and better temperature uniformity during the single discharge compared to the small simple design. The observed maximum temperature T_{av} and temperature uniformity ΔT were 22.2°C/1.2°C and 22.3°C/1.4°C for small simple and big simple designs respectively. Both models improved the isothermalisation of the cell compared to natural convection, where the maximum temperature T_{max} and temperature uniformity ΔT were 27.2°C/1.8°C Therefore, it can be concluded that the addition of PCM mass did not improve the cooling rate of the Li-Ion cells at DR=3C. Importantly, the higher thermal mass did not lead to better temperature uniformity. This might be as a result of the relatively low thermal conductivity of the PCM which could lead to the portion of PCM far from the cell to be thermally disconnected and therefore not used.

When tested under 10 consecutive charge-discharge cycles (Figure 5 lower) at CR=1C and DR=3C, performance differences between the “small” and the “big” can be discerned. The small design worked for three cycles while the big simple design for five cycles as the PCM was undergoing melting. Once the PCM was completely liquid, the cell temperature rose and kept oscillating in the range of 19°C-29°C and 19°C-27°C for small simple and big simple designs respectively.

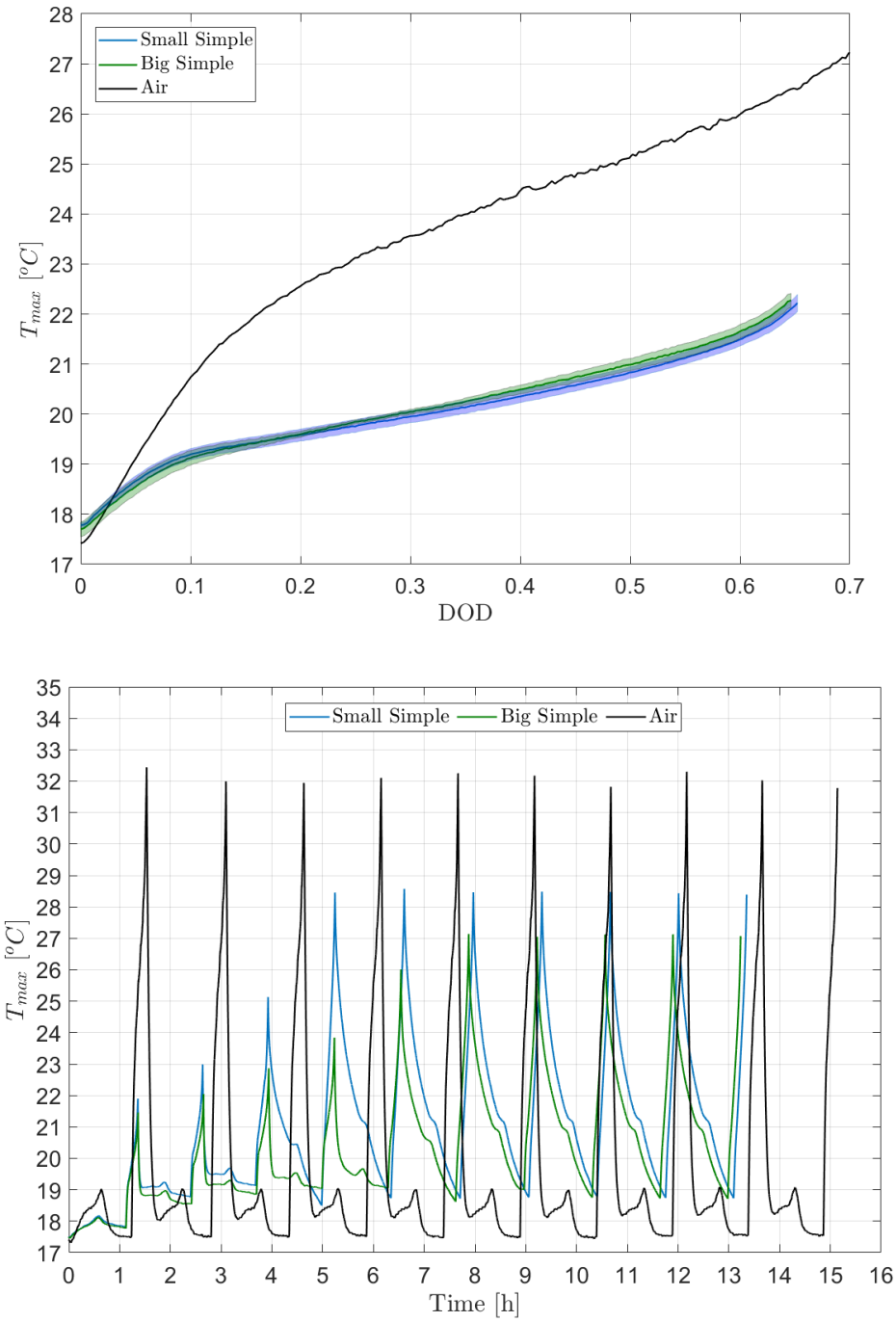

Figure 5: Effect of PCM DMLS TMS thermal mass (Small Simple vs Big Simple) on Li-Ion cell maximum temperature for single discharge at DR=3C (upper) and stress test comprising 10 consecutive cycles with charge at CR=1C and discharge at DR=3C (lower). The tests conducted with no dedicated TMS (i.e. air natural convection) is shown as a reference.

3.4 Combined effect of geometry and thermal mass

Similar data are reported in Figure 6 for two different geometry: small simple (blue) and big finned (yellow). The test conducted with no dedicated TMS (i.e. air natural convection) is also shown as a reference (black). As shown in Figure 2, the big finned design is characterised by a combination of the small finned and big simple

designs. A higher thermal mass is employed while the fins increase the equivalent thermal conductivity of the PCM, leading to a better thermal connection between the cell and the additional PCM. Overall, the big finned design leads to a lower maximum temperature (Figure 6 upper) and a better temperature uniformity during the single discharge compared to the small simple design. The observed maximum temperature T_{max} and temperature uniformity ΔT were 22.2°C/1.2°C and 21°C/1°C for small simple and big finned designs, respectively. Both models improved the isothermalisation of the cell compared to natural convection, where maximum temperature T_{max} and temperature uniformity ΔT were 27.2°C/1.8°C Therefore, it could be concluded that an increase of the PCM mass with a dedicated thermal conductivity enhancement element (i.e., fins) improved the cooling rate of the Li-Ion cells at DR=3C. Importantly, greater temperature uniformity was observed.

When tested under 10 consecutive charge-discharge cycles (Figure 5 lower) at CR=1C and DR=3C, the small design was observed to work in the phase transition stage for three cycles while the big finned design lasted for five cycles (similarly to the big simple). Once all solid PCM had been depleted, the cell temperature rose to a peak and oscillated in the range from 19°C-29°C and 19°C-27°C for small simple and big finned designs respectively.

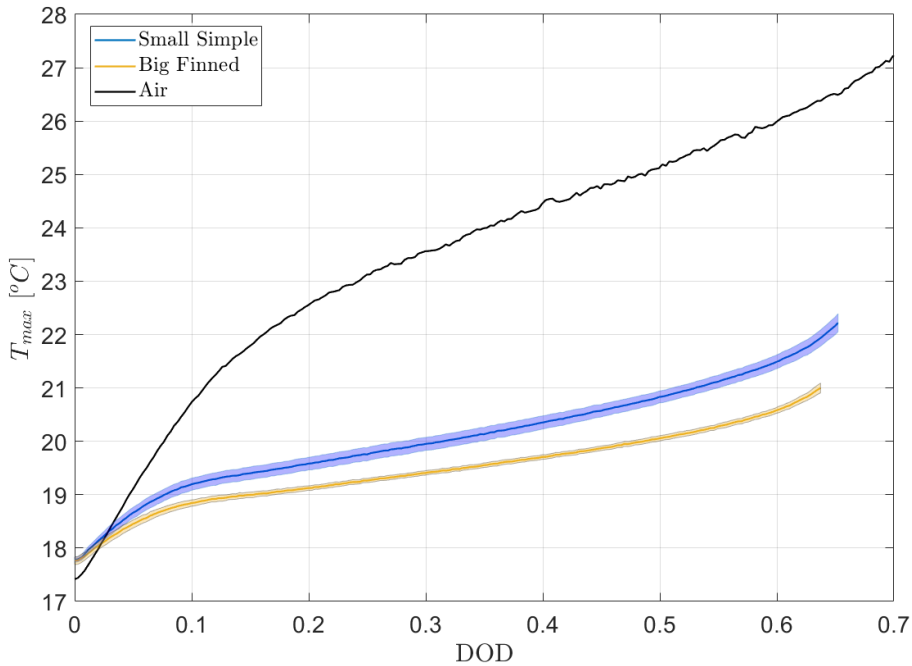

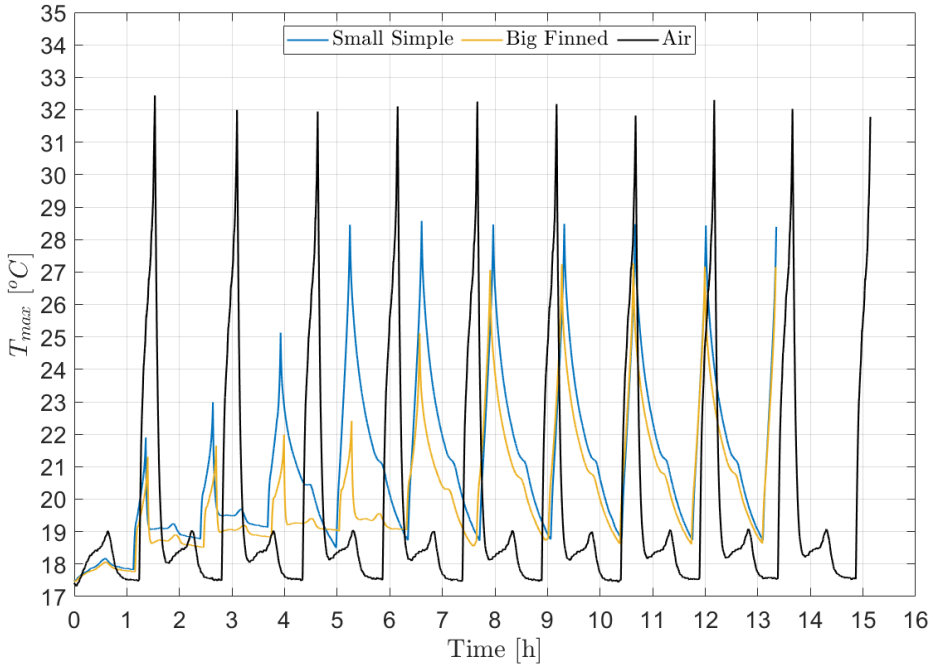

Figure 6: Combined effect of PCM DMLS TMS geometry and thermal mass (Small Simple vs Big Finned) on Li-Ion cell maximum temperature for single discharge at DR=3C (upper) and stress test comprising 10 consecutive cycles with charge at CR=1C and discharge at DR=3C (lower). The tests conducted with no dedicated TMS (i.e. air natural convection) is shown as a reference.

3.4. Overall Results

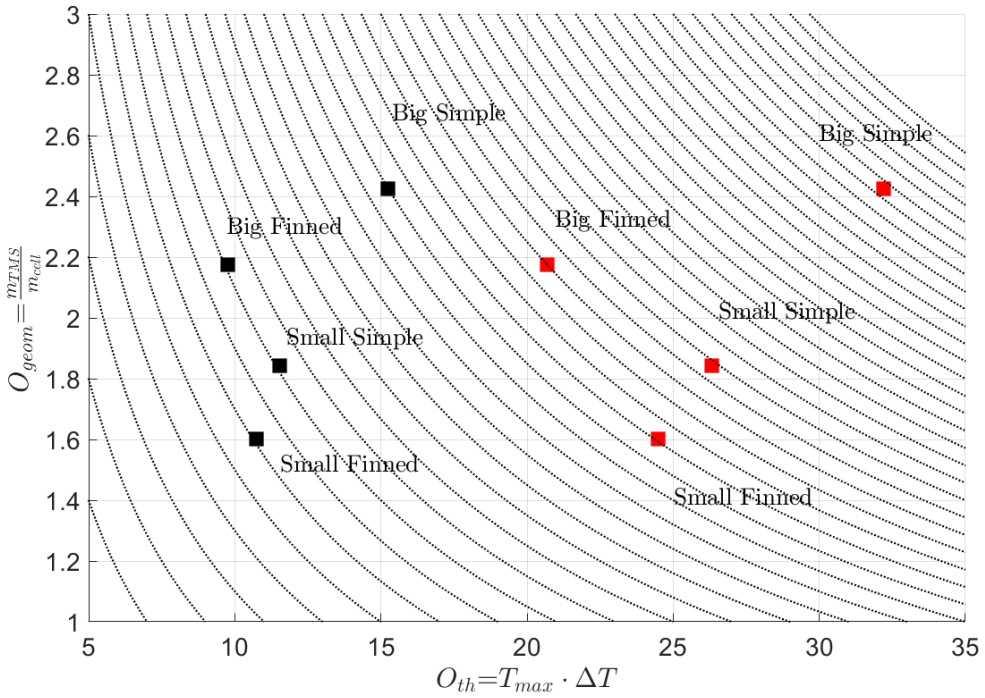

Figure 7: Pareto chart of overall results for single discharge tests. The definition of O_{th} can be based on the median (black squares) or the maximum (red squares) values of T_{max} and ΔT.

Figure 7 shows all PCM DMLS TMS designs' performance for the single discharge tests. These graphs are based on a Pareto front approach where two different objective functions to be minimised are defined: the thermal objective function O_{th} and the geometric objective function O_{geom}. O_{th} is defined as the product of the cell maximum temperature T_{max} and the cell temperature uniformity ΔT. As these quantities vary during a cell discharge test, the definition of O_{th} can be based on the median (black squares in Figure 7) or the maximum (red squares in Figure 7) values of T_{max} and ΔT. Instead, O_{geom} is simply defined as the ratio between the TMS mass (i.e., aluminium and PCM) and the cell mass, i.e. the additional weight due to the presence of a dedicated TMS. Besides, an overall objective O can be defined as the product of O_{th} and O_{geom} and iso-O can be drawn in the Pareto chart (black dotted lines in Figure 7). The optimal design could therefore be defined as the one that minimises O (in Figure 7 the closest to the origin of axis), i.e. represents the minimum temperature, better temperature uniformity, and at the same does not lead to excessive additional weight.

From the results reported in Figure 7, it can be claimed that the small finned design has the best performance when looking at either median (black) and maximum (red) values while the big simple result in less favourable overall performance. Interestingly, the big finned design results are better than the small simple design when looking at the maximum values while the contrary is true for median values. It can then be concluded that the small finned design guarantees the best thermal performance with minimal additional weight when looking at single discharges, i.e. intermittent loads.

Figure 8 shows all PCM DMLS TMS designs performance for the stress tests, i.e. 10 consecutive charge and discharge cycles at CR=1C and DR=3C. In this case, the definition of the thermal objective function O_{th} must be modified to include the transient behaviour of the PCM. All designs have a defined number of cycles after which the PCM is completely melted and therefore the TMS has minimal or no effect on the thermal management of the Li-Ion cell. Therefore, a new definition of O_{th} is used in this case where the number of cycles n_{cycle} is introduced as denominator in the definition of O_{th}. The definition of O_{geom} remains unvaried. The overall objective O is defined as the product of O_{th} and O_{geom} and iso-O are drawn in the Pareto chart (black dotted lines in Figure 7). The optimal design could therefore be defined as the one that guarantees the minimum O (in Figure 7 the closest to the origin of axis), i.e. guarantees the smallest temperature increase, the best temperature uniformity, limits the excessive additional weight, and lasts the highest number of equivalent cycles.

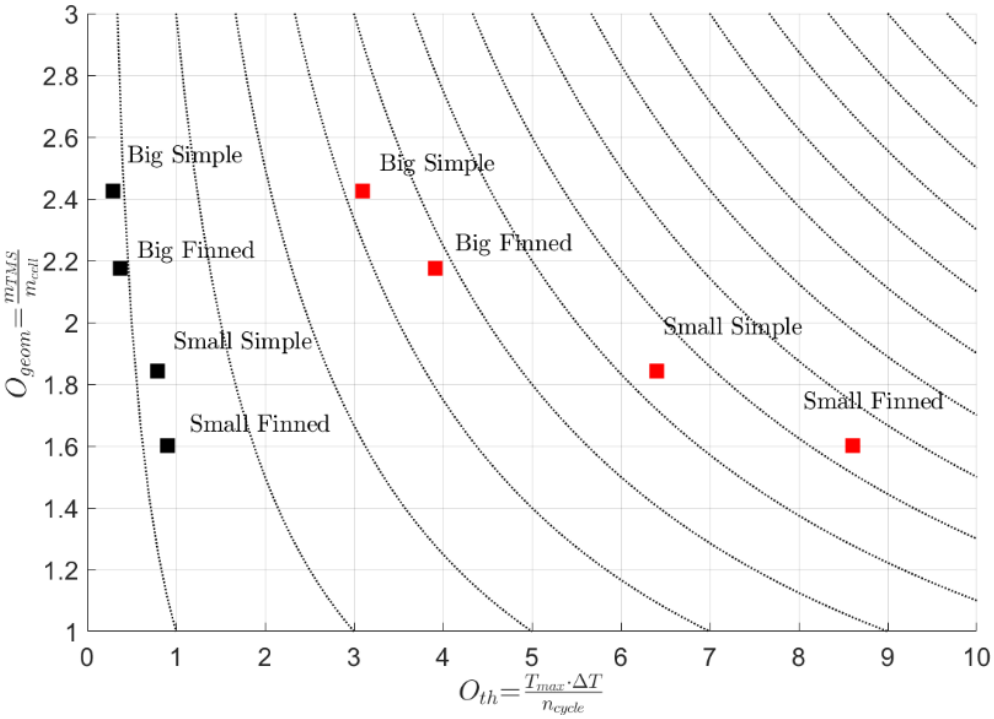

Figure 8: Pareto chart of overall results for stress tests. The definition of O_{th} can be based on the median (black squares) or the maximum (red squares) values of T_{max} and ΔT.

From the results reported in Figure 8, it can be claimed that both big designs have better performance compared to the small designs when looking at either median (black) and maximum (red) values. This is mainly since the big designs last 2 cycles more than the small ones, as evident in Figure 4, Figure 5, and Figure 6. Interestingly, the performances are not dissimilar when looking at the median values (black squares) while the differences are visible when looking at the maximum values (red squares). So, it can be concluded that the big designs guarantee the best thermal performance with reduced additional weight when looking at consecutive discharges, i.e. constant loads.

4. Conclusions

The present study evaluated some of the design parameters influencing the thermal performance of a TMS based on PCM. To do so, four different TMS designs with geometrical and thermal capacity variations were considered and experimentally tested using an established methodology and analysis procedure.

The blocks were produced using Direct-Metal-Laser-Sintering (DMLS) technique of two different sizes and geometrical variations, with and without fins embedded in the PCM pockets. Constant discharge rate tests and stress sequences were used to partially reproduce realistic cell operating conditions. Insulation around the block

allowed to reproduce the lack of convection inside a battery pack and were compared to the operation of the battery under natural convection conditions and no dedicated TMS.

The manufactured designs varied both in their thermal mass and geometry to assess the effects of increased thermal energy storage capacity and improved heat transfer performance of the TMS on the overall performance of the Li-Ion pouch cell.

Although both finned and simple designs proved to effectively improve the isothermalisation of the battery and decrease the overall maximum temperature by at least 5°C, the improved heat transfer performance of the finned design, however, proved to marginally improve the temperature uniformity by 0.1°C and decrease the maximum temperature by 0.8°C in the cell when compared to the simple design. However, for the stress tests, little to no difference was evident as in both cases the entire mass of PCM melted by the third cycle.

The effect of thermal mass was studied by comparing the two sizes of the simple design. When focusing on the single discharge tests, the additional PCM mass produced nearly no difference in terms of maximum temperature (22.2°C small simple, 22.3°C big simple), and temperature uniformity (1.2°C small simple, 1.4°C big simple) on the system, most likely explained by the low conductivity of the PCM. Consecutive tests proved, however, that the increased thermal storage capacity allowed to extend the operation for 5 charge-discharge cycles, two more than the smaller counterpart.

The combined effects were analysed by comparing the small simple and big finned designs. The finned design once again showed a better temperature uniformity (1.2°C small simple, 1°C big finned) as well as clear improvement on the maximum temperature of around 6°C. Additionally, the larger PCM mass allowed for its operation during 5 cycles.

Using the proposed Pareto front analysis and defined thermal and geometrical objectives, it is concluded that overall, the best compromise between thermal performance and reduced additional weight, when looking at both median and maximum values, is achieved by the small finned design for single discharge tests (i.e., intermittent load) and by both bigger designs for stress tests (i.e. constant load). This aspect is really important as in real applications not only the mass but also the volume are crucial aspects when it comes to real applications, especially for mobile devices. An investigation on the potentials to use alternative PCMs such as salt hydrates, characterised by higher specific latent heats and reduced volumes, would be valuable.

From the presented results it becomes apparent that no global optimum exists for the design of such a PCM-based, Li-Ion cell TMS. On the contrary, the selection of the HEX geometry and PCM mass but also of other important parameters such as the PCM melting temperature will have to be based on careful, application-specific considerations of several parameters. In addition, the stress tests highlighted the need for a hybrid TMS based on PCM and an additional active cooling strategy (e.g. air cooling, liquid cooling) to guarantee the isothermalisation of Li-Ion cells in applications where demanding charge/discharge cycles and limited resting periods are necessary. Therefore, as a next step, the authors aim to develop a numerical tool, which will be validated with the experimental data presented in this study, and will be used as a design tool in future works to determine suitable passive and hybrid TMS design configurations for a variety of Li-Ion cells battery pack types and application conditions.

Acknowledgement

The authors would like to express their gratitude to the Energy Technology Partnership (ETP) and the Swiss Competence Centre for Energy Research Storage of Heat and Electricity (SCCER) who funded this research.

References

[1] S. Landini, J. Leworthy, T.S. O'Donovan, A Review of Phase Change Materials for the Thermal Management and Isothermalisation of Lithium-Ion Cells, J. Energy Storage. 25 (2019). https://doi.org/10.1016/j.est.2019.100887.

[2] Z. Rao, S. Wang, A review of power battery thermal energy management, Renew. Sustain. Energy Rev. 15 (2011) 4554–4571. https://doi.org/10.1016/j.rser.2011.07.096.

[3] K. Shah, C. McKee, D. Chalise, A. Jain, Experimental and numerical investigation of core cooling of Li-ion cells using heat pipes, Energy. 113 (2016) 852–860. https://doi.org/10.1016/j.energy.2016.07.076.

[4] S. Landini, R. Waser, A. Stamatiou, R. Ravotti, J. Worlitschek, T.S. O'Donovan, Passive cooling of Li-Ion cells with direct-metal-laser-sintered aluminium heat exchangers filled with phase change materials, Appl. Therm. Eng. 173 (2020) 115238. https://doi.org/10.1016/j.applthermaleng.2020.115238.

[5] S. Landini, T.S. O'Donovan, Novel experimental approach for the characterisation of Lithium-Ion cells performance in isothermal conditions: Datasets and Supplementary Materials, Mendeley Data. (2020). https://doi.org/10.17632/fddsp6nnwd.1.

[6] T. Waldmann, M. Wilka, M. Kasper, M. Fleischhammer, M. Wohlfahrt-Mehrens, Temperature dependent ageing mechanisms in Lithium-ion batteries e A Post-Mortem study, J. Power Sources. 262 (2014) 129–135. https://doi.org/10.1016/j.jpowsour.2014.03.112.

[7] G. Vertiz, M. Oyarbide, H. Macicior, O. Miguel, I. Cantero, P. Fernandez De Arroiabe, I. Ulacia, Thermal characterization of large size lithium-ion pouch cell based on 1d electro-thermal model, J. Power Sources. 272 (2014) 476–484. https://doi.org/10.1016/j.jpowsour.2014.08.092.

[8] Z. Wang, X. Li, G. Zhang, Y. Lv, C. Wang, F. He, C. Yang, C. Yang, Thermal management investigation for lithium-ion battery module with different phase change materials, R. Soc. Chem. 7 (2017) 42909–42918. https://doi.org/10.1039/c7ra08181b.

[9] R. Kizilel, A. Lateef, R. Sabbah, M.M. Farid, J.R. Selman, S. Al-Hallaj, Passive control of temperature excursion and uniformity in high-energy Li-ion battery packs at high current and ambient temperature, J. Power Sources. 183 (2008) 370–375. https://doi.org/10.1016/j.jpowsour.2008.04.050.

[10] W.H. Zhu, H. Yang, K. Webb, T. Barron, P. Dimick, B.J. Tatarchuk, A novel cooling structure with a matrix block of microfibrous media / phase change materials for heat transfer enhancement in high power Li-ion battery packs, J. Clean. Prod. 210 (2019) 542–551.

https://doi.org/10.1016/j.jclepro.2018.11.043.

[11] A. Greco, X. Jiang, D. Cao, An investigation of lithium-ion battery thermal management using paraffin/porous-graphite-matrix composite, J. Power Sources. 278 (2015) 50–68. https://doi.org/10.1016/j.jpowsour.2014.12.027.

[12] N. Javani, I. Dincer, G.F. Naterer, G.L. Rohrauer, Modeling of passive thermal management for electric vehicle battery packs with PCM between cells, Appl. Therm. Eng. 73 (2014) 307–316. https://doi.org/10.1016/j.applthermaleng.2014.07.037.

[13] S. Landini, T.S. O'Donovan, Novel experimental approach for the characterisation of Lithium-Ion cells performance in isothermal conditions, Energy. 214 (2020) 118965. https://doi.org/10.1016/j.energy.2020.118965.

[14] L. Müller, G. Rubio-Pérez, A. Bach, N. Muñoz-Rujas, F. Aguilar, J. Worlitschek, Consistent DSC and TGA methodology as basis for the measurement and comparison of thermo-physical properties of phase change materials, Materials (Basel). 13 (2020) 1–20. https://doi.org/10.3390/ma13204486.